Thermally Activated Delayed Fluorescence in Fullerenes

CARLOS BALEIZÃO AND MÁRIO N. BERBERAN-SANTOS

Centro de Química-Física Molecular, Instituto Superior Técnico, Lisbon, Portugal

This report reviews the thermally activated delayed fluorescence (TADF) displayed by fullerenes. From the analysis of the steady-state data, time-resolved data, or by a combination of both, it is possible to determine several important photophysical parameters of fullerenes. Herein we also cover the development of temperature and oxygen sensors based on the TADF effect exhibited by fullerene C_{70}. Despite the work already carried out, knowledge of the photophysics of fullerenes and derivatives is still incomplete, and much remains to be done in this area and in the improvement of sensor systems based on fullerenes.

Key words: **fullerenes; C_{60}; C_{70}; thermally activated delayed fluorescence; temperature sensing; oxygen sensing**

Introduction

The discovery of fullerenes in 1985[1] and their production in macroscopic amounts after 1990[2] opened a new field of research. Applications of fullerenes in areas, such as energy, materials, biopharmaceuticals, optics, and electronics, have started to appear in recent years. The most common fullerenes are C_{60} and C_{70}, three-dimensional carbon structures that can be viewed either as large carbon molecules or as tiny nanoparticles with well-defined composition and shape. Their photophysical and photochemical properties result from the many delocalized π electrons present and from the high symmetry and curvature of the structures. The photophysics of fullerenes has been the subject of considerable investigation.[3–5] One of the most characteristic and (to us) interesting photophysical properties of C_{60}, C_{70}, and derivatives, first observed in our group, is a second mechanism for fluorescence, which is called thermally activated delayed fluorescence (TADF). This phenomenon, which occurs in a few fluorescent molecules, is usually weak; however, for fullerenes it is strong, especially for C_{70}. Herein, we briefly review the TADF of fullerenes and the development of temperature and oxygen sensors based on this property.

Address for correspondence: Mário N. Berberan-Santos, Centro de Química-Física Molecular, Instituto Superior Técnico, Av. Rovisco Pais, 1049-001 Lisbon, Portugal. Voice: +351-218419254; fax: +351-218464455.

berberan@ist.utl.pt

TADF: Fundamental Aspects

Two distinct unimolecular mechanisms exist for molecular fluorescence: prompt fluorescence (PF) and TADF.[6,7] In the PF mechanism, emission occurs after $S_n \leftarrow S_0$ absorption and excited state relaxation to S_1. The TADF mechanism takes place by way of the triplet manifold: After excitation and once S_1 is attained, intersystem crossing (ISC) to the triplet manifold (T_1 or a higher triplet) occurs, followed by a second ISC from T_1 back to S_1, and by fluorescence emission proper. The cycle $S_1 \rightarrow T_1 \rightarrow S_1$ may be repeated several times before fluorescence finally takes place. TADF is significant only when the quantum yield of triplet formation (Φ_T) and the quantum yield of singlet formation (Φ_S) are both high.[8] This outcome in turn implies a small energy gap between S_1 and T_1 (ΔE_{ST}), a long T_1 lifetime, and not too low a temperature.[8] For a given fluorophore, TADF is usually much weaker than its PF. Although known for many years, TADF continues to be a rare phenomenon, with a few observations in some xanthene dyes,[6,9,10] aromatic ketones[11,12] and thiones,[13,14] metal porphyrins,[15] and aromatic hydrocarbons.[16–18]

The remarkable photophysical properties of fullerene C_{70}, specifically for the Φ_T very close to 1,[19] the small ΔE_{ST} gap,[20] and the long intrinsic phosphorescence lifetime,[21] led to the discovery of an exceptionally strong TADF in this molecule.[8] C_{60}[22] and some C_{60} derivatives,[23,24] as well as one C_{70} derivative,[25] also exhibit TADF, but weaker than that of C_{70}.

The simplest model for TADF in the condensed phases is a three-state system that can be represented by

Ann. N.Y. Acad. Sci. 1130: 224–234 (2008).
doi: 10.1196/annals.1430.044

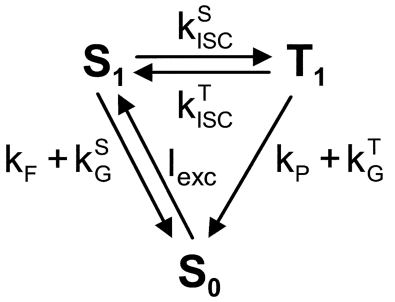

SCHEME 1. Kinetic scheme for TADF.

SCHEME 1,where I_{exc} is the excitation intensity; k_F and k_P are the radiative rate constants for fluorescence and phosphorescence, respectively; k^S_G and k^T_G are the nonradiative rate constants for deactivation to the ground state (internal conversion from S_1 and ISC from T_1, respectively); and k^S_{ISC} and k^T_{ISC} are the ISC rate constants for singlet-to-triplet and triplet-to-singlet conversion, respectively. Owing to the relative energies of S_1 and T_1, the triplet-to-singlet ISC rate constant always corresponds to an activated process that is strongly temperature dependent[6,8,26,27]:

$$k^T_{ISC} = A \exp\left(-\frac{\Delta E_{ST}}{RT}\right) \tag{1}$$

For strong TADF to occur, the following inequalities need to be met: $k^S_{ISC} \gg k_F + k^S_G$ and $k^T_{ISC} \gg k_P + k^T_G$. Usually it is also observed that $k^S_{ISC} \gg k^T_{ISC}$ and $k^T_G \gg k_P$.

The time evolution of the S_1 and T_1 populations is given by the following coupled equations,[28] where for simplicity the square brackets representing the concentrations are omitted:

$$S_1(t) = I_{exc}(t) \otimes \exp(-t/\tau_F) + k^T_{ISC}\, T_1(t) \otimes \exp(-t/\tau_F) \tag{2}$$

$$T_1(t) = k^S_{ISC}\, S_1(t) \otimes \exp(-t/\tau_P) \tag{3}$$

Here $\otimes$ stands for the convolution between two functions, $f \otimes g = \int_0^t f(u)\, g(t-u)\, du$; $\tau_F = 1/(k_F + k^S_G + k^S_{ISC})$ is the (prompt) fluorescence lifetime; and $\tau_P = 1/(k_P + k^T_G + k^T_{ISC})$ is called here the phosphorescence lifetime. These two lifetimes have direct experimental meaning only in the absence of reversibility; otherwise, fluorescence and phosphorescence no longer have single exponential decays, as will be discussed below. The low-temperature phosphorescence lifetime is $\tau^0_P = 1/(k_P + k^T_G)$. For rigid molecules, the temperature dependence of k^T_G is dictated mainly by external effects, that is, interactions with the solvent and other solutes present, such as oxygen and impurities, and therefore k^T_G is expected to change moderately with temperature in a deoxygenated and photochemically inert solid medium.[29]

SCHEME 1 is isomorphous to the monomer–excimer scheme (without transient effects[30]) and therefore has the same general solution. This solution can be obtained by inserting EQUATION (3) into EQUATION (2),

$$S_1(t) = I_{exc}(t) \otimes \exp(-t/\tau_F) + k^S_{ISC}\, k^T_{ISC}\, S_1(t) \otimes \exp(-t/\tau_P) \otimes \exp(-t/\tau_F) \tag{4}$$

and then by repeated substitution of the left-hand side on the right-hand side,[26]

$$\begin{aligned} S_1(t) = {} & I_{exc}(t) \otimes \exp(-t/\tau_F) \\ & + k^S_{ISC}\, k^T_{ISC}\, I_{exc}(t) \otimes \exp(-t/\tau_F) \otimes \exp(-t/\tau_P) \otimes \exp(-t/\tau_F) + \\ & + \left(k^S_{ISC}\, k^T_{ISC}\right)^2 I_{exc}(t) \otimes \exp(-t/\tau_F) \otimes \exp(-t/\tau_P) \otimes \exp(-t/\tau_F) \otimes \exp(-t/\tau_P) \otimes \exp(-t/\tau_F) + \ldots\ldots \end{aligned} \tag{5}$$

hence, the first term for the singlet decay can be associated with PF (zero $S_1 \to T_1 \to S_1$ cycles), and the remaining terms with delayed fluorescence, the nth term resulting from $n-1$ $S_1 \to T_1 \to S_1$ cycles. Analogous results can be obtained for the triplet decay. The singlet decay, EQUATION (5), simplifies into a sum of two exponentials of time, and the triplet decay into a difference of the same two exponentials[31]:

$$S_1(t) = \frac{S_1(0)}{\lambda_2 - \lambda_1}\left[(\lambda_2 - X)\exp(-\lambda_1 t) + (X - \lambda_1)\exp(-\lambda_2 t)\right] \tag{6}$$

$$T_1(t) = \frac{k^S_{ISC}\, S_1(0)}{\lambda_2 - \lambda_1}\left[\exp(-\lambda_1 t) - \exp(-\lambda_2 t)\right] \tag{7}$$

where

$$\lambda_{1,2} = \frac{1}{2}\left\{X + Y \mp \sqrt{(Y-X)^2 + 4\, k^S_{ISC}\, k^T_{ISC}}\right\} \tag{8}$$

with

$$X = \frac{1}{\tau_F} \tag{9}$$

and

$$Y = \frac{1}{\tau^0_P} + k^T_{ISC} \tag{10}$$

When interconversion between the singlet and triplet emissive states occurs many times before photon emission or nonradiative decay can take place, a fast preequilibrium between S_1 and T_1 is established, and

for sufficiently long times both S_1 and T_1 decay with a common rate constant given by[32]

$$k = \frac{k_{ISC}^{S}}{k_{ISC}^{S}+k_{ISC}^{T}} k_{G}^{T} + \frac{k_{ISC}^{T}}{k_{ISC}^{S}+k_{ISC}^{T}} k_{G}^{S} \qquad (11)$$

Given the inequalities mentioned, EQUATION (11) simplifies to

$$k = \frac{1}{\tau_{DF}} = k_{G}^{T} + (1-\Phi_T)\, k_{ISC}^{T} \qquad (12)$$

where Φ_T is the quantum yield of triplet formation, $\Phi_T = k_{ISC}^{S}/(k_F + k_G^S + k_{ISC}^S)$, and τ_{DF} is the delayed fluorescence (and phosphorescence) lifetime.

The fluorescence quantum yield is given by

$$\Phi_F = \Phi_{PF} + \Phi_{DF} \qquad (13)$$

where the quantum yields for prompt Φ_{PF} and delayed Φ_{DF} fluorescence obey the following relation[8]:

$$\frac{\Phi_{DF}}{\Phi_{PF}} = \frac{I_{DF}}{I_{PF}} = \frac{1}{\frac{1}{\Phi_S \Phi_T} - 1} \qquad (14)$$

and the quantum yield of singlet formation is defined by

$$\Phi_S = \frac{k_{ISC}^{T}}{k_P + k_G^T + k_{ISC}^T} \qquad (15)$$

In the high-temperature limit, $k_{ISC}^{T} \gg k_P + k_G^T$. Hence, $\Phi_S = \Phi_S^{\infty} = \frac{A}{k_P + k_G^T + A} \simeq 1$ (assuming that even in this range $A \gg k_G^T$), and EQUATION (14) becomes

$$\left(\frac{\Phi_{DF}}{\Phi_{PF}}\right)_{max} = \left(\frac{I_{DF}}{I_{PF}}\right)_{max} = \frac{1}{\frac{1}{\Phi_T} - 1} \qquad (16)$$

For strong TADF to occur, the cycle $S_1 \rightarrow T_1 \rightarrow S_1$ must repeat several times before photon emission or nonradiative decay can take place. To show this, it is convenient to present the TADF process as the following sequence (SCHEME 2):

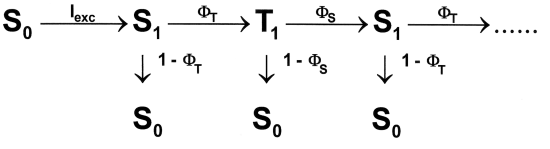

SCHEME 2. Sequential form for TADF. Taken from Ref. 26.

where the quantum yield of singlet formation is defined by EQUATION (15).

With this kinetic analysis, it is possible to determine several parameters. For example, the average number of cycles, $\bar{n}$, is given by

$$\bar{n} = \sum_{n=0}^{\infty} n\, p_n = \frac{\Phi_T \Phi_S}{1 - \Phi_T \Phi_S} = \frac{1}{\frac{1}{\Phi_T \Phi_S} - 1} = \frac{1}{\frac{1}{\Phi_T}\left(1 + \frac{1}{k_{ISC}^{T}\, \tau_P^0}\right) - 1} \qquad (17)$$

Comparison of EQUATIONS (17) and (14) gives immediately

$$\frac{\Phi_{DF}}{\Phi_{PF}} = \frac{I_{DF}}{I_{PF}} = \bar{n} \qquad (18)$$

and, using EQUATION (13),

$$\frac{\Phi_F}{\Phi_{PF}} = \frac{I_F}{I_{PF}} = 1 + \bar{n} \qquad (19)$$

hence, the increase in fluorescence intensity owing to TADF is a direct measure of the average number of $S_1 \rightarrow T_1 \rightarrow S_1$ cycles performed. This result is easy to understand, because each return from T_1 to S_1 brings a new opportunity for fluorescence emission.

Without reversibility, $\bar{n} = 0$. On the other hand, for the fastest possible excited state equilibration ($k_{ISC}^{T} \rightarrow A$, $\Phi_S \simeq 1$) one has

$$\bar{n} \simeq \frac{1}{\frac{1}{\Phi_T} - 1} \qquad (20)$$

Therefore, the maximum possible fluorescence intensification factor, EQUATION (19), is $1/(1 - \Phi_T)$.

Using the following set of data, obtained by our group for fullerene C_{70} dispersed in polystyrene[26,33,34]: $\Phi_T = 0.99$, $\tau_F = 630$ ps, $\tau_P^0 = 28$ ms, $A = 8 \times 10^7$ s^{-1}, $\Delta E_{ST} = 29$ kJ mol^{-1}, the maximum average number of cycles is estimated to be 99, and the maximum fluorescence intensification factor to be 100. The computed average number of cycles as a function of temperature is displayed in FIGURE 1. Many excited-state cycles are already effected at moderate temperatures.

Several methods of TADF data analysis exist. The classical one, from Parker,[6] combines steady-state delayed fluorescence and phosphorescence intensities for the determination of ΔE_{ST}. This method was successfully applied to C_{70}.[8] Nevertheless, measuring the phosphorescence is often not possible or convenient, and it is precisely in these cases that a nonspectroscopic method for the estimation of ΔE_{ST} becomes valuable. Furthermore, photophysical parameters other than ΔE_{ST} are of interest and can be extracted from experimental TADF data by other methods.

From the steady-state data, and for curve fitting, we can conveniently rewrite EQUATION (14) as[8]

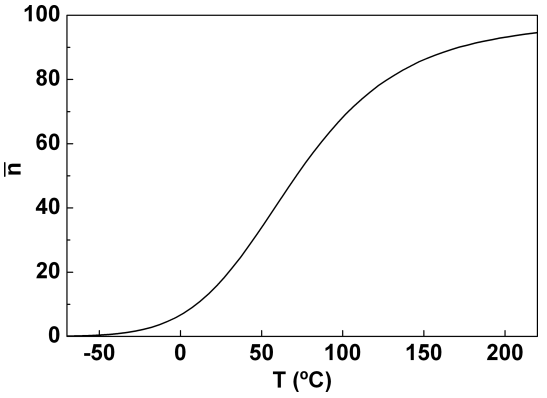

FIGURE 1. Computed average number of $S_1 \rightarrow T_1 \rightarrow S_1$ cycles as a function of temperature for C_{70} in polystyrene. Many excited-state cycles are already effected at moderate temperatures. From Ref. 26.

$$\ln\left[\frac{I_{PF}}{I_{DF}} - \left(\frac{1}{\Phi_T} - 1\right)\right] = \ln\left[\frac{1}{\Phi_T}\left(\frac{1}{\Phi_S^\infty} - 1\right)\right] + \frac{\Delta E_{ST}}{RT} \quad (21)$$

where

$$\Phi_S^\infty = \frac{1}{\frac{1}{A\tau_P^0} + 1} \quad (22)$$

and from a fit to steady-state data arranged in the above form[8] it is possible to recover ΔE_{ST}, Φ_T, and Φ_S^∞, assuming that Φ_S^∞ is temperature independent. Alternatively, a nonlinear curve fitting can also be carried out.

Concerning the time-resolved data, the time constant for the TADF lifetime is given by[26]

$$\lambda_1 = \frac{\frac{1}{\tau_P^0} + k_{ISC}^T(1 - \Phi_T)}{1 + k_{ISC}^T \tau_F} \quad (23)$$

and for $k_{ISC}^T \tau_F \ll 1$, as is usually the case, EQUATION (23) reduces to

$$\lambda_1 = \frac{1}{\tau_P^0} + k_{ISC}^T(1 - \Phi_T) \quad (24)$$

By using EQUATION (1), EQUATION (24) becomes

$$\lambda_1 = \frac{1}{\tau_P^0} + B \exp\left(-\frac{\Delta E_{ST}}{RT}\right) \quad (25)$$

where $B = (1 - \Phi_T)A$. From a nonlinear fit to the temperature dependence of the fluorescence long component (delayed fluorescence lifetime) using EQUATION (25), and assuming that τ_P^0 is temperature independent, it is possible to recover ΔE_{ST}, B, and τ_P^0 from time-resolved measurements. Nevertheless, and owing to parameter correlation, it is preferable to fix ΔE_{ST} at the steady-state value (obtained with EQUATION (21)). A and τ_P^0 can thus be extracted from the temperature dependence of the delayed fluorescence lifetime.[26] An alternative procedure is to rewrite EQUATION (25) as

$$\ln\left(\lambda_1 - \frac{1}{\tau_P^0}\right) = \ln B - \frac{\Delta E_{ST}}{RT} \quad (26)$$

and to search for the value of τ_P^0 that gives the best straight line.

A new method of analysis combines steady-state and time-resolved (delayed fluorescence) data in the same plot[26]:

$$\tau_{DF} = \tau_P^0 - \left(\frac{1}{\Phi_T} - 1\right)\tau_P^0 \frac{I_{DF}}{I_{PF}} \quad (27)$$

This linear plot yields Φ_T and τ_P^0, assuming τ_P^0 to be temperature independent. If τ_P^0 is already known, Φ_T can be directly obtained from EQUATION (27).

In conclusion, from steady-state and time-resolved data, it is in principle possible to obtain Φ_T, A, ΔE_{ST}, and τ_P^0 by using several methods.

Sensing Applications

The increasing need for continuous monitoring in areas as diverse as biotechnology, health care, environmental sciences, aerospace industry, nuclear industry, and marine sciences led to an increase of activity in the development of optical sensors beginning in the 1980s. Optical chemical sensors allow the continuous recording of the concentration of chemical species (e.g., O_2, CO_2, or several ions) and physical parameters (e.g., pressure, temperature) and therefore several applications have been found. Among the many optical methods that are used for sensing, fluorescence has attracted special attention because it is highly sensitive and versatile.[35]

In fluorescence, the sample can be both excited and measured optically. Therefore, fluorescence-based sensors, not requiring contact with the medium during measurement, are advantageous compared with contact sensors in applications where electromagnetic noise is strong or it is physically difficult to connect a wire. Further advantages of the molecular fluorescence sensors are the fast response, the reversibility, and the space resolution that can go from the macroscale (fluorescent paints) down to the nanoscale (fluorescence microscopy). These properties also overcome the limitations of electrochemical sensors (difficult to miniaturize, invasive technique, and limited to discrete points).

Temperature Measurement

Temperature is a basic property of matter, and its measurement is often required for both scientific research and industrial applications. Real-time temperature monitoring is of paramount importance in industrial testing and manufacturing and in many biomedical diagnostic and treatment processes. There are several thermal sensors based on molecular optical properties, namely, luminescence.[36] The use of fiber optics in conjugation with phosphors, whose luminescence lifetime changes with temperature, is a well-established method.[37] More recently, several studies have been devoted to fluorescence molecular thermometry,[38] including one molecular thermometer based on the fluorescence quenching of fullerene C_{60} dispersed in a polymer (polymethyl methacrylate) film.[39]

There is presently a need for optical sensors covering a wide temperature range, say, from 100°C to 250°C or even more. The common luminescence temperature sensors used currently are based on metallic complexes (e.g., Ru, Pt, Pd) whose intensities almost invariably decrease with a temperature increase owing to thermally activated quenching processes,[40] with working range temperatures below 100°C. The high thermal stability and the unique photophysical properties of fullerenes make these molecules well placed to fulfill this need.

The discovery[8] of the TADF in fullerene C_{70} was the first step for the development of temperature sensors based on the delayed fluorescence of fullerenes. The study was carried out in a degassed solution of liquid paraffin. The fluorescence spectra at different temperatures in degassed and nondegassed solutions are shown in FIGURE 2.[8]

The intensity of the nondegassed solution is independent of temperature and is entirely due to PF. The rise with temperature observed in the degassed solutions results from the increasing contribution of delayed fluorescence to the total intensity. The delayed fluorescence obtained at 70°C in degassed medium is 50 times stronger than the PF.

Fister *et al.*[41] demonstrated the use of the known delayed fluorescence of acridine yellow for the development of a molecular thermometer in the −50 to +50°C range. However, in contrast to C_{70}, the TADF of this compound is weak, which precludes fluorescence intensity measurements without the use of a time delay. Furthermore, the observed triplet decay is complex, preventing a clear interpretation of the results.

Other fullerenes molecules such as C_{60}[22] and some C_{60} derivatives,[23,24] as well as one C_{70} derivative,[25] also exhibit TADF, but not as strongly as C_{70} because of the high ΔE_{ST} and the lower Φ_T exhibited by these molecules. For example, for fullerene C_{60}, the global Φ_F can in principle be, at most, 10 times higher than that of PF,[22] whereas for fullerene C_{70} that value can be 167 times.[8]

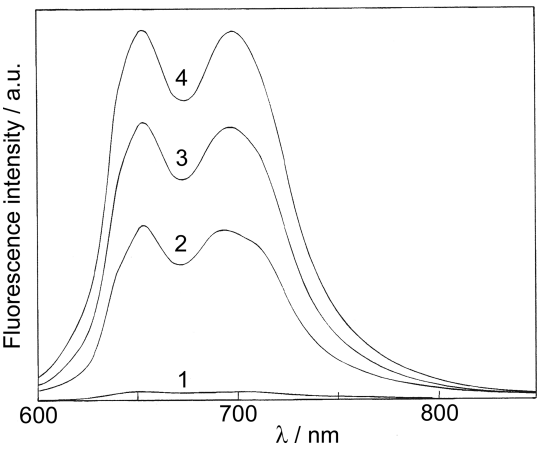

FIGURE 2. Temperature dependence of the fluorescence of a C_{70} solution in liquid paraffin. The emission of the aerated solution (1) is temperature independent, whereas a pronounced increase is observed upon degassing: 23°C (2), 50°C (3), and 70°C (4). Adapted from Ref. 8.

The reversibility of the C_{70}/paraffin system was also evaluated. Up to 70°C, the system shows total reversibility; however, for higher temperatures the reversibility is lost. Another drawback is the liquid nature of the system. For these reasons, we developed a series of polymer films with C_{70} molecularly dispersed in them.[33,34]

To study the influence of the polymer matrix structure on the photophysics and TADF of C_{70}, we selected three polymers: polystyrene (PS), poly(tert-butyl methacrylate) (PtBMA), and poly(1-vinylnaphthalene) (P1VN). The films were prepared by evaporating a toluene solution of C_{70} and polymer on a quartz plate. After film formation and drying, the plates were placed in a quartz cell that was degassed at room temperature and afterward sealed. All the films exhibited absorption spectra similar to that of C_{70} in toluene (for PS and P1VN) or methylcyclohexane (for PtBMA). These results are in agreement with a molecular dispersion of C_{70} in the polymeric films.

The fluorescence of the C_{70}/PS film at different temperatures and over a full heating–cooling cycle is shown in FIGURE 3. The first spectrum was recorded at room temperature (25°C) before degassing and corresponds to PF. Without degassing, the fluorescence intensity is temperature independent. After degassing, a 22-fold enhancement of the room-temperature fluorescence was observed. This enhancement is a

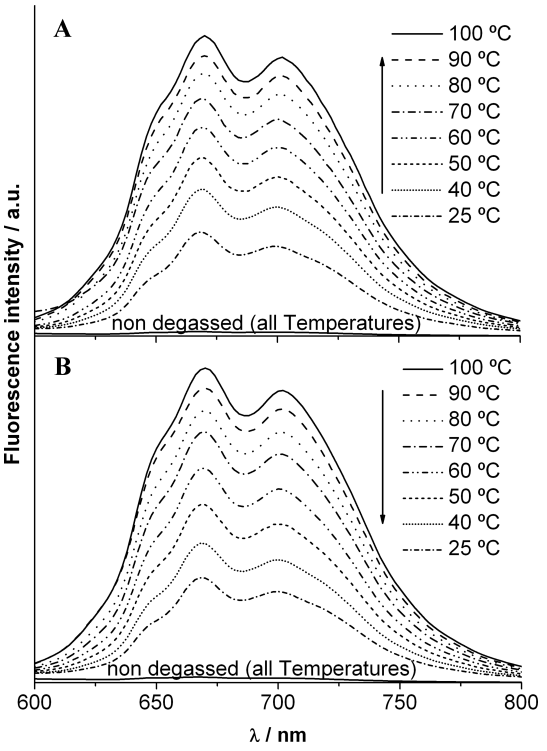

FIGURE 3. Fluorescence spectra ($\lambda_{exc} = 470$ nm) of a degassed C_{70}/PS film at different temperatures: **(A)** heating sequence (from 25 to 100°C); **(B)** cooling sequence (from 100 to 25°C). The emission of the nondegassed sample is also shown for comparison. Taken from Ref. 34.

consequence of the additional contribution of delayed fluorescence to the overall emission. Heating the sample to 100°C (FIG. 3A) (a temperature at which the delayed fluorescence is 70 times higher than the PF) shows that the fluorescence of C_{70} has a strong temperature dependence. The C_{70}/PS film exhibits full reversibility and fluorescence intensity cycles without hysteresis. The results exhibited a high degree of reproducibility.

The values of I_{DF}/I_{PF} for the C_{70}/PS film at different temperatures are collected in TABLE 1 and compared with the values previously measured for a solution of C_{70} in liquid paraffin.[8] The I_{DF}/I_{PF} ratios for the C_{70}/PS film are always higher than the values reported for C_{70} in paraffin. The values of I_{DF}/I_{PF} for the films were also measured over a wider temperature range than for C_{70} in paraffin. The stability of the C_{70}/PS after long-term storage is also high, with comparable ratios (<2% variation) of I_{DF}/I_{PF} being measured after several weeks of storage.

Identical temperature cycles were carried out for the C_{70}/P1VN and C_{70}/PtBMA films. Responses similar

TABLE 1. Experimental I_{DF}/I_{PF} (700 nm) for the C_{70} polymer systems for various temperatures

I_{DF}/I_{PF} (700 nm) system	25°C	50°C	70°C	100°C
C_{70}/paraffin[a]	20	35	50	—[b]
C_{70}/PS	22	39	53	70
C_{70}/P1VN	17	30	40	50
C_{70}/PtBMA	18	35	51	79

[a]Ref. 34.
[b]—, no data.

to that of the C_{70}/PS film were observed. The films exhibit good reversibility in the thermal cycles and high reproducibility. The I_{DF}/I_{PF} values for these films at several temperatures are also reported in TABLE 1. The maximum I_{DF}/I_{PF} value was obtained at 100°C with the C_{70}/PtBMA system.

The temperature sensitivity of fluorescence intensity was also calculated and can be defined either as the variation of the fluorescence quantum yield with temperature, which is the absolute sensitivity S_A (EQUATION (28)), or as the relative variation of the fluorescence quantum yield with temperature, which is the relative sensitivity S_R (EQUATION (29)).

$$S_A = \frac{d\Phi_F}{dT} \tag{28}$$

$$S_R = \frac{1}{\Phi_F}\frac{d\Phi_F}{dT} = \frac{d\ln\Phi_F}{dT} \tag{29}$$

We will use the relative sensitivity because it directly reflects the relative variation of the fluorescence intensity. The temperature dependence of S_R for the C_{70}/polymer systems is displayed in FIGURE 4. The C_{70}/polymer systems have some of the highest temperature sensitivities known over a broad temperature range.[42] To define a useful working range, we assume a minimum value of 0.5% K^{-1} for S_R. With this value, the lower temperature limit is −80°C for all polymers. At the other end of the scale, the C_{70}/PtBMA system displays the highest high-temperature limit (140°C), whereas for the other two polymers the upper limit is 110°C.

The performance of C_{70}/PtBMA was compared against ruthenium(II) polypyridyl complexes, which exhibit a strong temperature dependence. In particular, [Ru(phen)$_3$](tris(1,10- phenantroline)ruthenium) is a common optical temperature probe that displays efficient temperature quenching and high sensitivity. It is used because (1) it can be incorporated in solid matrices, such as sol-gels or polymers; (2) it is commercially available; (3) it is photostable; (4) it has a

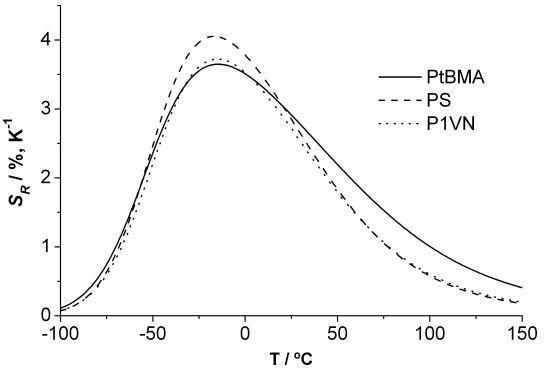

FIGURE 4. Relative variation in fluorescence S_R versus temperature for C_{70}/PtBMA (solid line), C_{70}/PS (dashed line), and C_{70}/P1VN (dotted line). Taken from Ref. 34.

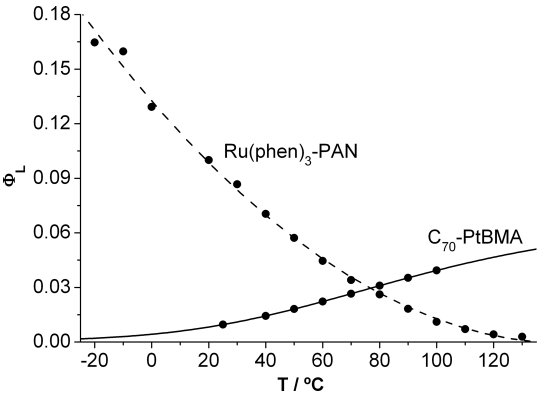

FIGURE 5. Temperature dependence of the luminescence quantum yields (Φ_L) of C_{70}/PtBMA (solid line) and [Ru(phen)$_3$]/PAN (dashed line). Experimental points are shown as circles. Taken from Ref. 34.

large Stokes shift; and (5) it can be excited in the visible region.[43] However, the luminescence of Ru(II) polypyridyl complexes is quenched by oxygen, and to avoid this interference in temperature sensing, we used poly(acrylonitrile) (PAN) as a matrix as a result of its very low gas permeability.[44] The temperature dependence of the luminescence quantum yields of C_{70}/PtBMA and [Ru(phen)$_3$]/PAN systems are shown in FIGURE 5. For temperatures higher than 80°C, the luminescence quantum yield of C_{70} in PtBMA exceeds that of [Ru(phen)$_3$]in PAN.

The C_{70}-based luminescence thermometer is a new development in the molecular thermometry field owing to the possibility of using a highly sensitive probe that covers not only both the low temperature and the physiological temperature ranges but also temperatures well above 100°C.

Oxygen Sensing

Oxygen, being essential for life, is an immensely important chemical species. Determination of oxygen levels is required in many different research areas. In medicine, oxygen levels in exhaled air or in the blood of a patient are key physiological parameters. Such parameters should ideally be monitored continuously. The measurement of oxygen levels is also essential in industries that use metabolizing organisms, such as yeast for brewing and baking, and in biotechnology, where microorganisms are used in the production of antibiotics and anticancer drugs.

Trace oxygen detection is important from a safety standpoint,[45] because oxygen leaks can cause fires and explosions and can be harmful in storage chambers and packaged food[46] and in aerospace research.[47] Common trace oxygen sensors are based on amperometry (Clark electrodes). These are sensitive and applicable over a wide temperature range but are difficult to miniaturize, invasive, and limited to discrete points.[48]

Optical sensors do overcome these limitations. Recently, a variety of devices and sensors based on molecular optical properties have been developed to measure oxygen partial pressure on the solid surface. Many optical oxygen sensors are composed of organic dyes, transition metal complexes, and metalloporphyrins immobilized in oxygen-permeable materials.[49] There is still a need for optical sensors that can respond to low levels of oxygen. The sensitivity to oxygen of excited fullerenes was observed in the triplet–triplet quenching of fullerene polymeric films by using laser flash photolysis.[50] The TADF effect in the fullerenes is sensitive to the presence of oxygen,[8] leading to an efficient quenching of the intensity and lifetime of TADF. Because of this ultrasensitivity to oxygen, fullerenes are good candidates for sensing oxygen in low concentrations.

In a recent report, fullerene C_{70} was embedded in two highly permeable polymer membranes, an organosilica and an ethyl cellulose, and used as optical sensor for trace amounts of oxygen with detection limits in the part-per-billion volume (ppbv) range.[51]

The highest O_2 permeabilities are displayed by silica-based polymers. But in all reports of sol-gels doped with unfunctionalized fullerenes, the fullerene was partially aggregated owing to formation of small clusters.[52] These aggregates show largely reduced fluorescence intensities and lifetimes as a result of self-quenching. We have been able to incorporate C_{70} into an organically modified silica (OS) without significant aggregation by using a monomer where one alkoxy group is replaced by a phenyl ring.[52] Organosilicas are less polar and thus more compatible with fullerenes.[53,54] Ethyl cellulose 49%

TABLE 2. Stern–Volmer constants and detection limits for delayed fluorescence quenching of C_{70} in OS and EC, respectively, by O_2 at various temperatures and comparison with the literature

Probe	T (°C)	K_{SV1}/(mg (O_2)/L)$^{-1}$	Detection limit/(ppmv (O_2))	Ref.
C_{70} /OS	0	25.1	0.34	51
	20	28.4	0.30	51
	60	26.0	0.32	51
	120	15.1	0.54	51
C_{70} /EC	0	47.0	0.18	51
	20	52.9	0.16	51
	60	36.1	0.23	51
	120	16.9	0.48	51
PdOEP/silica	20	3.74	2.44	58
PtOEP/silica	20	0.37	25.26	58
PtTFPP/silica	20	0.12	77.88	58
PtTPP/silica	20	0.17	57.38	58
$Ru(dpp)_3$/silica	20	3.2×10^{-2}	400.27	58
PdTFPP/PTBS	20	1.32	6.87	55
PdTFPP/EC	20	1.27	6.42	55
PdTFPP/EC[a]	20	1.12	7.35	55
PtTFPP/PTBS	20	0.13	77.31	55
PtTFPP/EC	20	0.18	51.41	55
$Ru(dpp)_3$/PTBS	20	1.4×10^{-2}	776.33	55

Taken from Ref. 51

[a]EC with 46% ethylation; PdOEP: palladium octaethylporphyrin; PdTFPP: palladium tetrapentafluorophenylporphyrin; PtOEP: platinum ocatethylporphyrin; PTBS: poly (4-tert)butyl styrene; PtTFPP: platinum tetrapentafluorophenylporphyrin; PtTPP: platinum tetraphenylporphyrin; Ru(dpp)3: ruthenium tris-(4,7)-diphenylphenanthroline.

(EC) also is a highly permeable matrix for oxygen sensing.[55] C_{70} is compatible with this matrix. The absence of significant aggregation was demonstrated through the absorption spectra, lifetime measurements, atomic force microscopy, and scanning electron microscopy.[51]

We investigated the sensitivity to oxygen by time domain fluorescence lifetime imaging.[56] The delayed fluorescence lifetimes exceed 20 ms in the absence of oxygen at room temperature and below and result in an extreme sensitivity to oxygen. The response is instantaneous (<0.1 s). The best fits for the Stern–Volmer plots were obtained by applying the two-site quenching model.[57] The fluorescence is most pronounced at 120°C, and C_{70} still shows delayed fluorescence lifetimes greater than 5 ms. The temperature dependence of the sensitivity is therefore the result of the following three effects upon increasing temperature: (1) increasing Φ_{DF}, (2) decreasing delayed fluorescence lifetime, and (3) higher collision rate of O_2. The Stern–Volmer constants depend on temperature in a nonlinear way, and both systems display detection limits (defined at 1% quenching) more than one order of magnitude better than state-of-the-art probes (TABLE 2).

The response of the matrices is fully reversible over many hundreds of times and showed no detectable degradation after 3 months of storage at room temperature in the dark on air. In conclusion, we developed an optical oxygen sensor that is especially suited for sensing oxygen down to the ppbv range and at high temperatures. The method makes use of the TADF of fullerene C_{70} dissolved in appropriate polymers. It enables, for the first time, the optical sensing and imaging of oxygen at the ppbv level, and thus has a large potential.

Concluding Remarks and Future Perspectives

This report reviewed selected results of our work in fullerene photophysics, with an emphasis on TADF. We showed that fullerenes display a strong TADF effect, which can be used to determine several photophysical parameters. This effect also allows the use of fullerenes as temperature and oxygen optical sensors under extreme conditions (high temperatures [>100°C] or low oxygen concentration [<1 part-per-million volume (ppmv)]).

Despite the work already carried out, knowledge of the photophysics of fullerenes and derivatives is still incomplete, and much remains to be done in this area and in optical sensor systems incorporating fullerenes.

The development of new materials with ultralow (or even zero) oxygen permeability and high thermal

stability (several hundreds of degrees) are needed to improve the optical temperature sensor materials based on fullerenes and TADF. These materials will bypass the drawback of working under vacuum, which is mandatory for using TADF as the mechanism of detection.

For optical sensors, another issue that should be given attention is the sensing of rare gases. The photophysics of fullerenes is affected by the external heavy-atom effect, such as that of bromine and iodine,[59,60] and it is expected that rare gases like krypton and xenon will have similar quenching properties.

The synthesis and preparation of new host–guest supramolecular assemblies, incorporating fullerenes and gold nanoparticles, has been subject of interest in the last few years.[61] These materials are especially suited for light–energy conversion systems. However, metal nanoparticles (e.g., those made of gold and silver) can tune the luminescence of fluorophores.[62,63] These variations are highly dependent on the diameter of the nanoparticles or type of surface[64] and can in principle be used in more complex sensor systems for multiparameter analysis.

Efforts should be made to obtain new compounds and materials based on fullerenes and nanoparticles to measure relevant physical parameters and analytes under favorable conditions.

Acknowledgments

This work was supported by Fundação para a Ciência e a Tecnologia (FCT, Portugal) and POCI 2010 (FEDER) within project POCI/QUI/58535/2004. C. Baleizão was supported through fellowship SFRH/BPD/28438/2006. Collaboration with the group of O. S. Wolfbeis (Institute of Analytical Chemistry, Chemo-, and Biosensors, University of Regensburg, Germany) is gratefully acknowledged.

Conflict of Interest

The authors declare no conflicts of interest.

References

1. Kroto, H.W. *et al*. 1985. C_{60}—buckminsterfullerene. Nature **318:** 162–163.
2. Krätschmer, W. *et al*. 1990. Solid C_{60}—a new form of carbon. Nature **347:** 354–358.
3. Foote, C.S. 1994. Photophysical and photochemical properties of fullerenes. Top. Curr. Chem. **169:** 347–363.
4. Sun, Y.P. 1997. Photophysics and photochemistry of fullerene materials. *In* Molecular and Supramolecular Photochemistry, Vol. 1, Organic Photochemistry. V. Ramamurthy & K.S. Shanze, Eds.: 325–390. Marcel Dekker. New York.
5. Sun, Y.P. *et al*. 2000. Photoexcited state and electron transfer properties of fullerenes and related materials. *In* Optical and Electronic Properties of Fullerenes and Fullerene-Based Materials. J. Shinar, Z.V. Vardeny & Z.H. Kafafi, Eds.: 43–81. Marcel Dekker. New York.
6. Parker, C.A. 1968. Photoluminescence of Solutions. Elsevier. Amsterdam.
7. Valeur, B. 2002. Molecular Fluorescence: Principles and Applications. Wiley-VCH. Weinheim.
8. Berberan-Santos, M.N. & J.M.M. Garcia. 1996. Unusually strong delayed fluorescence of C_{70}. J. Am. Chem. Soc. **118:** 9391–9394.
9. Lam, S.K. & D. Lo. 1997. Time-resolved spectroscopic study of phosphorescence and delayed fluorescence of dyes in silica-gel glasses. Chem. Phys. Lett. **281:** 35–43.
10. Duchowicz, R., M.L. Ferrer & A.U. Acuña. 1998. Kinetic spectroscopy of erythrosin phosphorescence and delayed fluorescence in aqueous solution at room temperature. Photochem. Photobiol. **68:** 494–501.
11. Wolf, M.W. *et al*. 1975. Photophysical studies on the benzophenones. Prompt and delayed fluorescences and self-quenching. J. Am. Chem. Soc. **97:** 4490–4497.
12. Turek, A.M. *et al*. 2002. Resolution of benzophenone delayed fluorescence and phosphorescence with compensation for thermal broadening. J. Phys. Chem. A **106:** 6044–6052.
13. Maciejewski, A., M. Szymanski & R.P. Steer. 1986. Thermally activated delayed S1 fluorescence of aromatic thiones. J. Phys. Chem. **90:** 6314–6318.
14. Eisenberger, H. & B. Nickel. 1996. Photophysical triplet state processes of 4-H-1-benzopyrane-4-thione in a perfluoroalkane. Part 1.—Temperature dependence of unimolecular triplet decay. J. Chem. Soc. Faraday Trans. **92:** 733–740.
15. Yusa, S., M. Kamachi & Y. Morishima. 1998. Photophysical behavior of zinc(II) tetraphenylporphyrin covalently incorporated in a cholesterol-bearing polymethacrylate. Photochem. Photobiol. **67:** 519–525.
16. Kropp, J.L. & W.R. Dawson. 1967. Radiationless deactivation of triplet coronene in plastics. J. Phys. Chem. **71:** 4499–4506.
17. Nickel, B. & D. Klemp. 1993. The lowest triplet state of azulene-h_8 and azulene-d_8 in liquid solution. I. Survey, kinetic considerations, experimental technique, and temperature dependence of triplet decay. Chem. Phys. **174:** 297–318.
18. Nickel, B. & D. Klemp. 1993. The lowest triplet state of azulene-h_8 and azulene-d_8 in liquid solution: II. Phosphorescence and E-type delayed fluorescence. Chem. Phys. **174:** 319–330.
19. Arbogast, J.W. & C.S. Foote. 1991. Photophysical properties of C_{70}. J. Am. Chem. Soc. **113:** 8886–8889.
20. Argentine, S.M., K.T. Kotz & A.H. Francis. 1995. Temperature and solvent effects on the luminescence spectrum of C_{70}: assignment of the lowest singlet and triplet states. J. Am. Chem. Soc. **117:** 11762–11767.

21. Wasielewski, M.R. *et al*. 1991. Triplet states of fullerenes C_{60} and C_{70}. Electron paramagnetic resonance spectra, photophysics, and electronic structures. J. Am. Chem. Soc. **113:** 2774–2776.
22. Salazar, F.A., A. Fedorov & M.N. Berberan-Santos. 1997. A study of thermally activated delayed fluorescence in C_{60}. Chem. Phys. Lett. **271:** 361–366.
23. Gigante, B. *et al*. 1999. Diels-Alder adducts of C_{60} and resin acid derivatives: synthesis, electrochemical and fluorescence properties. Tetrahedron **55:** 6175–6182.
24. Anthony, S.M., S.M. Bachilo & R.B. Weisman. 2003. Comparative photophysics of $C_{61}H_2$ isomers. J. Phys. Chem. A **104:** 10674–10679.
25. Bachilo, S.M. *et al*. 2000. Time-resolved thermally activated delayed fluorescence in C_{70} and 1,2-$C_{70}H_2$. J. Phys. Chem. A **104:** 11265–11269.
26. Baleizão, C. & M.N. Berberan-Santos. 2007. Thermally activated delayed fluorescence as a cycling process between excited singlet and triplet states: application to the fullerenes. J. Chem. Phys. **126:** 204510.
27. Tanaka, F., M. Okamoto & S. Hirayama. 1995. Pressure and temperature dependences of the rate constant for S1-T2 intersystem crossing of anthracene compounds in solution. J. Phys. Chem. **99:** 525–530.
28. Berberan-Santos, M.N. & J.M.G. Martinho. 1992. A linear response approach to kinetics with time-dependent rate coefficients. Chem. Phys. **164:** 259–269.
29. Graves, W.E., R.H. Hofeldt & S.P. McGlynn 1972. Temperature dependence of phosphorescence characteristics of aromatic hydrocarbons in poly(methylmethacrylate). J. Chem. Phys. **56:** 1309–1314.
30. Berberan-Santos, M.N. & J.M.G. Martinho. 1991. Diffusion-influenced excimer formation kinetics. J. Chem. Phys. **95:** 1817–1824.
31. Birks, J.B. 1970. Photophysics of Aromatic Molecules. Wiley. London.
32. Rae, M. & M.N. Berberan-Santos. 2002. Pre-equilibrium approximation in chemical and photophysical kinetics. Chem. Phys. **280:** 283–293.
33. Baleizão, C. & M.N. Berberan-Santos. 2006. A molecular thermometer based on the delayed fluorescence of C_{70} dispersed in a polystyrene film. J. Fluoresc. **16:** 215–219.
34. Baleizão, C. *et al*. 2007. Optical thermometer based on the delayed fluorescence of C_{70}. Chem. Eur. J. **13:** 3643–3651.
35. Wolfbeis, O.S. 2004. Optical technology until the year 2000: an historical overview. *In* Optical Sensors for Industrial, Environmental and Clinical Applications. R. Narayanaswamy & O.S. Wolfbeis, Eds.: 1–34. Springer. Berlin.
36. Uchiyama, S., A.P. de Silva & K. Iwau. 2006. Luminescent molecular thermometers. J. Chem. Educ. **83:** 720–727.
37. Grattan, K.T. & Z.Y. Zhang. 1995. Fiber Optic Fluorescence Thermometry. Chapman and Hall. London.
38. Lou, J.F. *et al*. 1999. Fluorescence-based thermometry: Principles and applications. Rev. Anal. Chem. **18:** 235–284.
39. Amao, Y. & I. Okura. 2002. Optical molecular thermometer based on the fluorescence of fullerene dispersed in poly(methyl methacrylate) film. Bull. Chem. Soc. Jpn. **75:** 389–391.
40. Demas, J.N. & B.A. DeGraff. 2001. Applications of luminescent transition platinum group metal complexesto sensor technology and molecular probes. Coord. Chem Rev. **211:** 317–351.
41. Fister III, J.C., D. Rank & J.M. Harris. 1995. Delayed fluorescence optical thermometry. Anal. Chem. **67:** 4269–4275.
42. Wolfbeis, O.S. 2004. Fiber-optic chemical sensors and biosensors. Anal. Chem. **76:** 3269–3284.
43. Liebsch, G., I. Klimant & O.S. Wolfbeis. 1999. Luminescence lifetime temperature sensing based on sol-gels and poly(acrylonitrile)s dyed with ruthenium metal-ligand complexes. Adv. Mater. **11:** 1296–1299.
44. Brandrup, J., E.H. Immergut & E.A. Grulke. 1999. Permeability and diffusion data. *In* Polymer Handbook. Wiley. New York.
45. Denison, D.M. *et al*. 1968. Problem of fire in oxygen-rich surroundings. Nature **218:** 1110–1113
46. Mills, A. 2005. Oxygen indicators and intelligent inks for packaging food. Chem. Soc. Rev. **34:** 1003–1011.
47. Seife, C. 2003. NASA's hypersonic lab studies factors leading to breakup. Science **299:** 1971.
48. Ramamoorthy, R., P.K. Dutta & S.A. Akbar. 2003. Oxygen sensors: materials, methods, designs and applications. J. Mater. Sci. **38:** 4271–4282.
49. Amao, Y. 2003. Probes and polymers for optical sensing of oxygen. Mikrochim. Acta **143:** 1–12.
50. Amao, Y., K. Asai & I. Okura. 1999. Optical oxygen pressure sensing based on triplet–triplet quenching of fullerene–polystyrene film using laser flash photolysis: soccerballene C_{60} versus rugbyballene C_{70}. Bull. Chem. Soc. Jpn. **72:** 2223–2227.
51. Nagl, S. *et al*. 2007. Optical sensing and imaging of trace oxygen with record response. Angew. Chem. Int. Ed. Engl. **46:** 2317–2319.
52. Brusatin, G. & P. Innocenzi. 2001. Fullerenes in sol-gel materials. J. Sol-Gel Sci. Technol. **22:** 189–204.
53. Klimant, I. *et al*. 1999. Fast response oxygen micro-optodes based on novel soluble Ormosil glasses. Mikrochim. Acta **131:** 35–46.
54. Jaroniec, M. 2006. Materials science: organosilica the conciliator. Nature **442:** 638–640.
55. Apostolidis, A. *et al*. 2004. A combinatorial approach for development of materials for optical sensing of gases. J. Comb. Chem. **6:** 325–331.
56. Lin, Z. *et al*. 2004. Fluorescent imaging of citrate and other intermediates in the citric acid cycle. Angew. Chem. Int. Ed. Engl. **43:** 1735–1738.
57. Demas, J.N. & B.A. DeGraff. 1995. Modeling of luminescence quenching-based sensors: comparison of multisite and nonlinear gas solubility models. Anal. Chem. **67:** 1377–1380.
58. Han, B.H., I. Manners & M.A. Winnik. 2005. Oxygen sensors based on mesoporous silica particles on layer-by-layer self-assembled films. Chem. Mater. **17:** 3160–3171.
59. Rae, M. *et al*. 2006. Intra- and intermolecular heavy-atom effects on the fluorescence properties of brominated C_{60} polyads. J. Phys. Chem. B **110:** 12809–12814.
60. Foley, S. *et al*. 2001. Effect of halogenated compounds on the photophysics of C_{70} and a monoadduct of C_{70}: some

implications on optical limiting behaviour. Chem. Phys. **263:** 437–447.

61. IMAHORI, H. *et al*. 2005. Host–guest interactions in the supramolecular incorporation of fullerenes into tailored holes on porphyrin-modified gold nanoparticles in molecular photovoltaics. Chem. Eur. J. **11:** 7265–7275.
62. ASLAN, K. *et al*. 2007. Fluorescent core-shell Ag@SiO_2 nanocomposites for metal-enhanced fluorescence and single nanoparticle sensing platforms. J. Am. Chem. Soc. **16:** 55–62.
63. ASLAN, K., S.N. MALYN & C.D. GEDDES 2007. Metal-enhanced fluorescence from gold surfaces: angular dependent emission. J. Fluoresc. **17:** 7–13.
64. ASLAN, K. *et al*. 2005. Metal-enhanced fluorescence: an emerging tool in biotechnology. Curr. Opin. Biotech. **16:** 55–62.